Kyushu University Global COE Program
Journal of Novel Carbon Resource Sciences, Vol. 2, pp. 17-20, Sep. 2010

LEED analysis of graphite films on vicinal 6H-SiC(0001) surface

Kenjiro Hayashi[*1#], Seigi Mizuno[*1] and Satoru Tanaka[*2]

[*1]Department of Molecular and Material Sciences, Kyushu University
[*2]Department of Applied Quantum Physics and Nuclear Engineering, Kyushu University
[#]Present address: Fujitsu Laboratories Ltd., 10-1 Morinosato-Wakamiya, Atsugi, Kanagawa 243-0197, Japan

(Received June 11, 2010; accepted September 16, 2010)

We studied the stacking sequence of graphite films formed by the thermal decomposition of a vicinal (tilted 4° toward the [11$\bar{2}$0] direction) 6H-SiC(0001) substrate surface. Thin (typically three layers) graphite films grown by annealing at 1400 °C or 1500 °C showed clear low-energy electron diffraction (LEED) patterns with a threefold rotational symmetry. This indicates that one of two equivalent domains of graphite films is dominantly grown on the vicinal surface. The quantitative LEED analysis determined that thick (~10 layers) graphite films formed after annealing at 1900 °C exhibited Bernal (AB…) stacking preferentially. On the other hand, a sixfold rotational symmetry was found on the flat (not inclined) sample surface after annealing at 1400 °C due to mixed rotational domains and various graphite thicknesses. These results show that better-quality graphite films were achieved on the vicinal surface than on the flat surface.

1. Introduction

Thin graphite films, i.e. few-layer graphenes, have attracted much attention as potentially good candidates for future electronic devices due to their unique capabilities, including their anomalous quantum Hall effect, long coherent length, and ballistic conductivity[1-4]. While thin graphite films have been prepared by mechanical exfoliation of highly oriented pyrolitic graphite (HOPG), this method has limitations in terms of the size and scope of production. On the other hand, epitaxial growth of graphite films has been achieved on silicon carbide (SiC) surfaces, and is based on a solid-state graphitization by annealing of SiC in a vacuum[5]. This method has the potential to lead to high-quality graphite films up to the SiC substrate size; thus, it appears to be a promising route for the fabrication of large-scale graphite films. Many researches have been approached with the view of improving the domain size and homogeneity of graphite films on the SiC surface[6-12]. On flat 6H-SiC(0001) substrates, however, graphite films were found by Hibino *et al*. to have large thickness distributions, based on low-energy electron microscopy (LEEM)[13-15]. In addition, Ohta *et al*. measured electronic band structures corresponding to the number of graphene layers on the flat substrate surface by means of angle-resolved photoemission spectroscopy (ARPES), which clarified that tri- and quadlayer graphite films consist of mixtures of different stacking sequences, i.e. Bernal (AB…) and rhombohedral (ABC…) stackings[16]. The electronic properties of thin graphite films, which essentially govern the functions of electronic devices, are expected to be influenced by the stacking sequence as well as the number of graphene layers[17]. Therefore, the control of these structural parameters is a crucial issue for the development of graphene-based nanoelectronics.

Meanwhile, vicinal SiC surfaces are expected to obtain relatively uniform graphite films since step-flow like growth of graphite films preferentially progresses on them if surface decompositions occur from their step edges. In this study, we investigated the surface symmetry and determined the stacking sequence of graphite films grown on a vicinal SiC(0001) substrate by means of quantitative low-energy electron diffraction (LEED).

2. Experiments

Samples used in this study were commercially available vicinal (4° toward the [11$\bar{2}$0] direction) and flat 6H-SiC(0001) substrates. The samples were washed with ethanol and acetone in an ultrasonic bath, before being loaded into a cold-wall horizontal reactor. H_2 gas etching was then performed at 1340 °C for 30 min under atmospheric pressure to remove residual polishing damage on the surfaces. The resulting vicinal surface showed nanofacet structures consisting of pairs of (0001) terraces and (11$\bar{2}n$) facets[18,19].

The samples were loaded into an ultra-high- vacuum (UHV) chamber (< 7 × 10^{-9} Pa) equipped with LEED. Surface graphitization was carried out at a temperature of 1400 °C, 1500 °C, or 1900 °C for 30 min (< 5 × 10^{-6} Pa), and LEED patterns were observed in each case. LEED spot intensities were acquired by a computer-controlled video camera system at normal electron incidence geometry[20]. Intensity versus energy curves [*I(E)*-curves] of graphite (1 × 1) LEED patterns were measured in the incident energy range of 70-400 eV. A Barbieri-Van Hove symmetrized automated tensor LEED package was used in dynamical LEED calculation to generate theoretical *I(E)*-curves[21] based on structure models. Thirteen phase shifts were used to represent atomic scattering. The incident electron attenuation was represented by the imaginary part of the inner potential V_{0i} of -4.5 eV. A comparison of experimental data and theoretical *I(E)*-curves was carried out by the Pendry R-factor (R_P); a smaller R_P meant better agreement[22]. Errors in the structural parameters were estimated by the variance of R_P, $\Delta R = R_P(8 \mid V_{0i} \mid /\Delta E)^{1/2}$.

3. Results and discussion

Figures 1(a) and (b) show LEED patterns obtained on the vicinal SiC(0001) surface after annealing at 1400 °C and 1500 °C, respectively. We observed clear graphite (1 × 1) patterns with a threefold rotational symmetry at several energy ranges, indicating that one of two equivalent rotating domains of graphite films is dominantly grown on the surface and that those thicknesses are relatively uniform. Wu et al. reported similar threefold rotational symmetry on a (0001) face of a cleaved natural graphite crystal, which was interpreted as a result of a single termination (i.e. little or no atomic steps) on the surface[23]. Thermal decomposition on the vicinal surface is expected to occur from step edges and to progress as layer-by-layer growth of graphite films, which leads to relatively uniform thickness. On a flat SiC(0001) surface after annealing at 1400 °C, however, a sixfold rotational symmetry was observed on the LEED pattern as shown in Fig. 1(d). As reported in previous studies[6-8], equal amounts of two rotational domains exist on the surface. The LEED pattern of a $(6\sqrt{3} \times 6\sqrt{3})R30°$ reconstruction was also observed over the whole energy range. The $(6\sqrt{3} \times 6\sqrt{3})R30°$ structure is commonly observed in the initial stages of surface graphitization[9,11,12], and it is believed that a buffer layer is located at the interface between the undermost graphite film and SiC substrate[9,24,25]. The graphite films fabricated on the flat surface are thus expected to have varying thickness distributions including domains that are thinner than that on the vicinal surface.

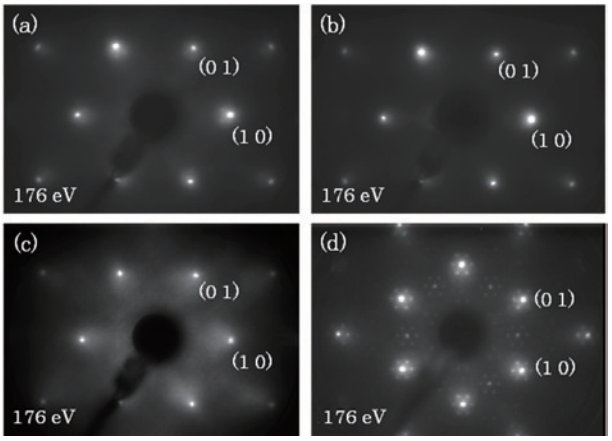

Fig. 1 (a)-(c) LEED patterns obtained on the vicinal SiC(0001) surface after annealing at 1400, 1500 and 1900 °C, respectively. (d) A LEED pattern obtained on the flat SiC(0001) surface after annealing at 1400 °C.

Figure 2(a) shows experimental *I(E)*-curves of (1 0), (0 1), (2 0) and (0 2) spots of graphite films. Several significant differences were obtained between the curves of (1 0) and (0 1) spots at incident electron energies of 100 eV, 176 eV and 330 eV, while the overall shape of the *I(E)*-curves showed similar features. The features of *I(E)*-curves of (2 0) and (0 2) spots also showed a significant difference of peak positions at 320 eV. Such differences due to the threefold rotational symmetry can be similarly found in theoretical *I(E)*-curves of each diffraction spot calculated for a model of a single graphite crystal, as shown in Fig. 2(b), indicating that the graphite films on the vicinal surface had essentially a single termination as reported previously[23]. However, our thin graphite films probably contain rotational domains in some degree, considering the fact that a difference of peak positions between (1 0) and (0 1) around 176 eV was smaller in the experimental than in the theoretical results, as shown in Figs. 2(a) and (b). This might have been caused by a mixture of *I(E)*-curves from majority and minority domains.

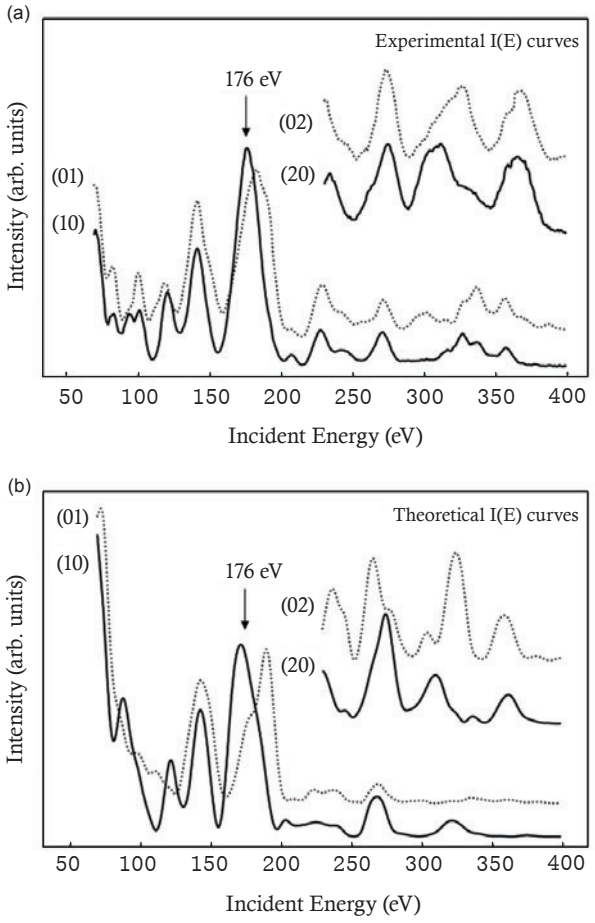

Fig. 2 Experimental and theoretical *I(E)*-curves of the vicinal SiC(0001) surface after annealing at 1400 °C.

While a single-layer-graphene sheet has six-fold rotational symmetry, a several-layer-graphene sheet has three-fold rotational symmetry if it has an AB stacking. There are two possible surface terminations, with an A or B layer. Since both surface terminations have the same surface energy, there are equal probabilities to appear on the flat surface. If there is a reason for preferential growth of one termination or if a single graphene sheet covers a huge area, a single termination will be observed.

We suppose the former to be operative in the present case. Our vicinal 6H-SiC(0001) surface has a uniform nanofacet structure[18]. The nanofacet consists of six or three SiC bilayer steps. The steps on the surface might play an important role in the formation process of graphite films because it is expected that surface decomposition occurs from the step edges[26]. Therefore, preferential termination might originate from the direction of the steps. This could be the reason for the single termination preferentially appearing on the vicinal surface. Similar results have been also obtained on the 6H-SiC(0001) surface covered with a layer of silicon oxynitride[27].

As the annealing temperature increases, the experimental *I(E)* curve features changed. Graphite films formed after further annealing at 1900 °C showed a sixfold rotational symmetry and the $(6\sqrt{3} \times 6\sqrt{3})R30°$ pattern was no longer visible in the LEED pattern, as shown in Fig. 1(c). We analyzed stacking sequences of the graphite films using a quantitative LEED method. Single graphite crystals were used for the model calculation without consideration of the SiC substrate and the interfacial buffer layer because of the thick graphite films. The stacking sequences of the graphite models were AB and ABC stackings. An equal ratio of rotational domains of the graphite crystal (double domain model) was assumed in each model. The experimental and theoretical *I(E)* curves are shown in Fig. 3 with resultant values of R_P for each curve. While the overall shapes of the theoretical *I(E)* curves of the (1 0) spot showed similar features due to their similar structures, the AB stacking model had better agreement with the experimental results. Better agreements between the experimental and theoretical results of (1 1) and (2 0) spots were also obtained for the AB stacking that gave an R_P of 0.16, whereas the ABC stacking had a larger R_P value of 0.22 as summarized in Table 1. The difference between the R_P values is remarkable considering the ΔR of 0.03, which indicates that thick graphite films grown on the vicinal surface have an AB stacking preferentially.

We also performed structural analysis on thin graphite films formed at 1400 °C and 1500 °C annealing. In these cases we made artificial *I(E)* curves with sixfold rotational symmetry by mixing the majority and minority domains. For example, we averaged the experimental (1 0) and (0 1) *I(E)* curves and compared them with the theoretical curves of double-domain models. In the calculations, we used two types of models: a single crystal model as used in the analysis of the thick graphite films and a trilayer graphite film model. The trilayer graphite film is separated from a bulk graphite crystal by a 10-nm-thick vacuum. The vacuum region attenuates the electron beams completely because we are using the imaginary part of the inner potential to represent damping, and the damping starts from the topmost surface layer. Therefore, the calculated *I(E)* curves of the latter model include information about the trilayer graphite film only. The trilayer graphite film was observed experimentally on the vicinal SiC substrates after annealing at 1400 °C for 30 min by transmission electron microscopy (TEM) and LEEM[27]. The obtained Pendry R-factors are summarized in Table 1. While we could obtain rather small R_P of 0.19-0.21 for samples annealed at 1400 °C and 1500 °C, there were no significant differences between the two stacking models. We also tried bi- and quad-layer graphite films but there were no improvements. Therefore, we could not determine the stacking sequence of the thin graphite films. An interfacial buffer layer and the SiC substrate were expected to make some contributions to the experimental *I(E)* curves since a $(6\sqrt{3} \times 6\sqrt{3})R30°$ pattern was observed at high incident electron energies even after annealing at 1500 °C. Actually, agreement of the experimental and theoretical *I(E)* curves was worse at higher incident electron energies than that at lower energies. The exact treatment of the interface layer in the calculation is difficult because of its huge unit cell.

On the other hand, the calculations for the flat surface

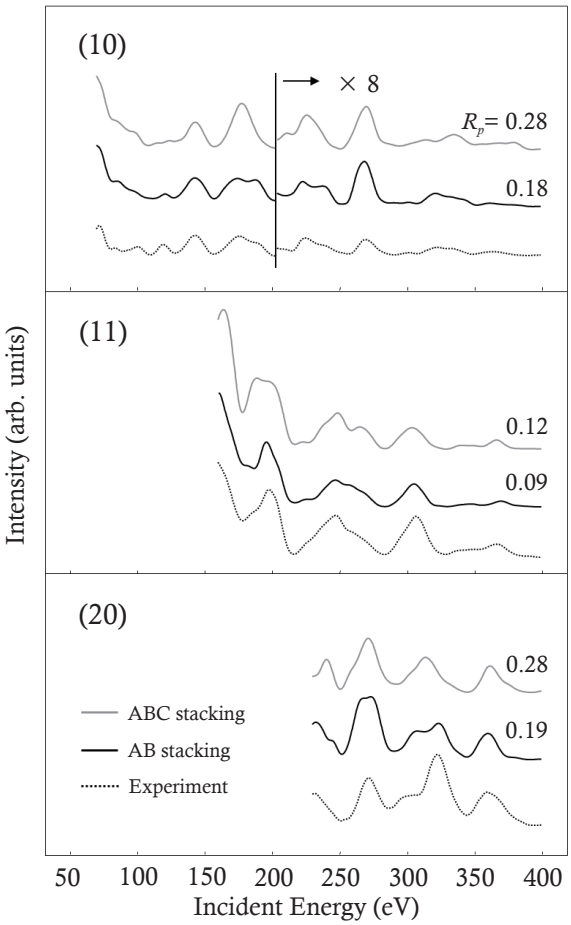

Fig. 3 Experimental and theoretical *I(E)*-curves of the flat SiC(0001) surface after annealing at 1900 °C.

Table 1 Pendry R-factors obtained on the vicinal and flat SiC(0001) surfaces after annealing

	Stacking	1400 °C	1500 °C	1900 °C
Vicinal	AB	0.21	0.20	0.16
	ABC	0.21	0.19	0.22
Just	AB	0.27		
	ABC	0.31		

assuming the single graphite crystal and trilayer models resulted in R_P values of 0.26-0.27 for the AB stacking and 0.28-0.30 for the ABC stacking. These larger R_P values might be caused by larger thickness distributions[13] and the mixture[16] of different stacking sequences as reported previously.

We clarified that thin graphite films on a vicinal surface have essentially a single termination. The quantitative LEED analysis clarified that thick graphite films with AB stacking are preferentially grown on such a surface. Vicinal surface fabrication, therefore, has the potential to result in high-quality graphite films compared to flat surface fabrication with respective to homogeneity in thickness and stacking sequence.

4. Conclusion

We studied the stacking sequence of graphite films formed on a vicinal 6H-SiC(0001) surface. After annealing at 1400 °C and 1500 °C, LEED patterns of thin graphite films showed a threefold rotational symmetry on the vicinal surface, but a sixfold rotational symmetry on the flat surface. These results indicate preferential growth of one of two rotational domains on the vicinal surface, while both domains are mixed in equal amounts on the flat surface. Considering such a difference depending on surface inclination, steps on the surface might play an important role in the formation process of graphite films. After further annealing at 1900 °C, thick graphite films formed on the vicinal surface, and the LEED patterns changed to a sixfold rotational symmetry. Our quantitative LEED analysis revealed that the graphite films preferentially adopted AB stacking on the vicinal SiC surface. The present results suggest that the vicinal substrate orientation is suitable in preparing uniform graphite films on an SiC surface.

Acknowledgement: This study was supported by KAKENHI (20340077) from the Ministry of Education, Culture, Sports, Science and Technology of Japan and the Industrial Technology Research Grant Program in ’05 from NEDO of Japan.

References

1) K.S. Novoselov, A.K. Geim, S.V. Morozov, D. Jiang, Y. Zhang, S.V. Dubonos, I.V. Grigorieva and A.A. Firsov, *Science*, **306**, 666 (2004).
2) Y. Zhang, Y.-W. Tan, H.L. Stormer, P. Kim, *Nature*, **438**, 201 (2005).
3) Claire Berger, Zhimin Song, Xuebin Li, Xiaosong Wu, Nate Brown, Cécile Naud, Didier Mayou, Tianbo Li, Joanna Hass, Alexei N. Marchenkov, Edward H. Conrad, Phillip N. First, Walt A. de Heer, *Science*, **312**, 1191 (2006).
4) A.K. Geim and K.S. Novoselov, *Nature Mater.*, **6**, 183 (2007).
5) A. J. Van Bommel, J. E. Crombeen and A. Van Tooren, *Surf. Sci.*, **48**, 463 (1975).
6) J. Hass, R. Feng, T. Li, X. Li, Z. Zong, W. A. de Heer, P. N. First, E. H. Conrad, C. A. Jeffrey, C. Berger, *Appl. Phys. Lett.*, **89**, 143106 (2006).
7) C. Berger, Z. Song, X. Li, X. Wu, N. Brown, C. Naud, D. Mayou, T. Li, J. Hass, A. N. Marchenkov, E. H. Conrad, P. N. First, and W. A. de Heer, *Science*, **312**, 1191 (2006).
8) K-J. Kim, H. Lee, J-H. Choi, H-K. Lee, T-H. Kang, B. Kim, and S. Kim, *J. Phys.: Condens. Matter*, **20**, 225017 (2008).
9) C. Riedl, U. Starke, J. Bernhardt, M. Franke, and K. Heinz, *Phys. Rev. B*, **76**, 245406 (2007).
10) T. Ohta, A. Bostwick, Th. Seyller, K. Horn, and E. Rotenberg, *Science*, **313**, 951 (2006)
11) Th. Seyller, K. V. Emtsev, K. Gao, F. Speck, L. Ley, A. Tadich, L. Broekman, J. D. Riley, R. C. G. Leckey, O. Rader, A. Varykhalov, and A. M. Shikin, *Surf. Sci*., **600**, 3906 (2006).
12) P. Lauffer, K. V. Emtsev, R. Graupner, Th. Seyller, L. Ley, S. A. Reshanov, H. B. Weber, *Phys. Rev. B*, **77**, 155426 (2008).
13) H. Hibino, H. Kageshima, F. Maeda, M. Nagase, Y. Kobayashi and H. Yamaguchi, *Phys. Rev. B*, **77**, 075413 (2008).
14) C. Riedl, A.A. Zakharov, and U. Starke, *Appl. Phys. Lett*., **93**, 033106 (2008).
15) T. Ohta, F. E. Gabaly, A. Bostwick, J. L. McChesney, K. V. Emtsev, A. K. Schmid, T. Seyller, K. Horn, and E. Rotenberg, *New J. Phys*., **10**, 023034 (2008).
16) T. Ohta, A. Bostwick, J. L. McChesney, T. Seyller, K. Horn, and E. Rotenberg, *Phys. Rev. Lett*., **98**, 206802 (2007).
17) M. Aoki, H. Amawashi, *Solid State Communications*, **142**, 123 (2007).
18) H. Nakagawa, S. Tanaka and I. Suemune, *Phys. Rev. Lett*., **91**, 226107 (2003).
19) M. Fujii and S. Tanaka, *Phys. Rev. Lett*., **99**, 016102 (2007).
20) S. Mizuno, T. Shirasawa, Y. Shiraishi and H. Tochihara, *Phys. Rev. B*, **69**, 241306 (2004).
21) M. A. Van Hove, W. Moritz, H. Over, P. J. Rous, A. Wander, A. Barvieri, N. Materer, U. Starke, and G. A. Somorjai, *Surf. Sci. Rep.*, **19** (1993) 191.
22) J. B. Pendry, *J. Phys. C*, **13**, 937 (1980).
23) N. J. Wu, and A. Ignatiev, *Phys. Rev. B*, **25**, 2983 (1982).
24) W. Norimatsu, M. Kusunoki, *Chem. Phys. Lett.*, **468**, 52 (2009).
25) H. Kageshima, H. Hibino, M. Nagase, and H. Yamaguchi, *Appl. Phys. Exp.*, **2**, 065502 (2009).
26) S. Tanaka, K. Morita, and H. Hibino, *Phys. Rev. B*, **81**, 041406 (2010).
27) K. Hayashi, K. Morita, S. Mizuno, H. Tochihara and S. Tanaka, *Surf. Sci.*, **603**, 566-570 (2009).